Relevance of quantum fluctuations in the Anderson-Kondo model

Robert Peters and Thomas Pruschke

Institute for Theoretical Physics, University of Göttingen,
Friedrich-Hund-Platz 1, 37077 Göttingen, Germany

We study a localized spin coupled to an Anderson impurity to model the situation found in higher transition metal or rare earth compounds like e.g. LaMnO$_3$ or Gd monopnictides. We find that, even for large quantum numbers of the localized spin, quantum fluctuations play an essential role for the case of ferromagnetic coupling between the spin and the impurity levels. For antiferromagnetic coupling, a description in terms of a classical spin is appropriate.

I. INTRODUCTION

Transition metal oxides show a fascinating complex behavior in their electronic properties.[1] This complexity stems from the interplay between the formation of narrow 3d-bands leading to a delocalization of these states on the one hand and the local part of the Coulomb interaction between the 3d-electrons tending to localize them.[1] While compounds of the early 3d elements like e.g. LaTiO$_3$, which typically accommodate one 3d electron, can at least qualitatively be described in terms of a one-band Hubbard model[2,3,4], materials involving higher transition metal elements like LaMnO$_3$ or TlSr$_2$CoO$_5$ require the use of a model including the full 3d shell. In particular, to understand the magnetic properties and the frequently occurring metal-insulator transitions[1] one has to take into account the interplay between density-("Hubbard U") and exchange-type ("Hund's J") contributions to the local Coulomb interaction. Note that similar features can also be found in compounds involving higher rare earth elements, for example the rare earth pnictides.

A particularly interesting example is La$_{1-x}$Ca$_x$MnO$_3$. Besides is complicated phase diagram comprising a large variety of paramagnetic and magnetically ordered metallic and insulating phases one finds a colossal magneto-resistance (CMR).[5] In this cubic perovskite the five-fold degenerate 3d level is split by crystal field into three-fold degenerate t_{2g}, which have the lower energy, and two-fold degenerate e_g states. These states have to be filled with $4 - x$ electrons, nominally yielding a metal even for $x = 0$. However, taking into account the local Coulomb interaction, three of these electrons will occupy the t_{2g}-states forming an $S = 3/2$ high-spin state due to Hund's coupling, which interacts ferromagnetically with the electron occupying the e_g states. Ignoring the Coulomb repulsion among the electrons in the e_g subsystem, one encounters the well-known double-exchange model[6], which has been extensively studied as suitable model for manganites (see e.g. references in Ref. 7). In most of these investigations, however, the t_{2g}-spin was approximated by a classical moment to allow the use of standard techniques like e.g. quantum Monte-Carlo[8,9,10,11,12,13,14] (QMC). Without such a replacement, one is typically restricted to low-order diagrammatic techniques (Ref. 15 and references therein).

A more realistic treatment should of course also include the local Coulomb interaction within the e_g subsystem. Such a model has been proposed recently[7] and studied in the framework of the dynamical mean-field theory[16] (DMFT). Again, the t_{2g}-spin had to be replaced by a classical moment to allow the solution of the DMFT equations with QMC.

In this paper we want to study the validity of approximating the quantum spin by a classical object. To this end, we investigate the simplest possible model, viz a quantum impurity model consisting of a local orbital with interacting charge degrees of freedom coupled to a non-interacting host and a spin.

While such a model surely cannot access every aspect of the physics of the corresponding lattice model, it is the basic ingredient in a DMFT calculation and thus understanding its fundamental properties is of importance to properly interpret results obtained in a DMFT calculation. Moreover, although such a calculation will focus on local dynamics only, one can obtain at least qualitative results about possible ordered phases, too.[16] To this end it is viable to obtain a feeling how the additional spin will modify local charge and spin properties.

We employ Wilson's numerical renormalization group[17,18] (NRG) to solve this model. This technique allows to treat the model in the whole parameter regime and in particular identify small energy scales if present.

The paper is organized as follows. In the next section we present the model and briefly review its properties for a classical spin in the limit of vanishing Coulomb interaction. The presentation of our results follows in section III. The paper closes with a summary and discussion.

II. THE MODEL

The simplest model that allows to obtain an idea how the coupling to an additional local spin-degree of freedom

influences the properties of correlated electrons is

$$H = \sum_{k\sigma} \epsilon_k c_{k\sigma}^\dagger c_{k\sigma} + \sum_\sigma \left(\epsilon_d + \frac{U}{2} d_{-\sigma}^\dagger d_{-\sigma} \right) d_\sigma^\dagger d_\sigma \quad (1)$$

$$+ \frac{V}{\sqrt{N}} \sum_{k\sigma} \left(c_{k\sigma}^\dagger d_{k\sigma} + \text{h.c.} \right)$$

$$- J_K \sum_{\alpha,\beta} \vec{S} \cdot \vec{s}_d \ .$$

The first three terms represent a conventional single-impurity Anderson model,[19,20] while the last contribution introduces an additional spin degree of freedom which couples to the local states via an exchange interaction. Similar models have been studied with various techniques in connection with double quantum dots.[21,22,23,24,25,26] However, in these cases the additional impurity was represented by a correlated charge degree of freedom coupled via a hopping. In the limit of half-filling and weak interimpurity hopping, this system maps to our model with $S = 1/2$ and vanishing antiferromagnetic J_K. This limit shows interesting physics on its own,[25,27] for example two-stage Kondo screening or quantum phase transitions. However, these models neither do allow for *ferromagnetic* J_K, large and possibly anisotropic J_K nor spins $S > 1/2$, which are the particular cases we are interested in here.

Of course our model (1) does not fully represent the situation found in e.g. LaMnO$_3$ since it lacks the orbital degrees of freedom. On the other hand, NRG calculations for multi-orbital models are extremely expensive[28] and we believe that as far as the qualitative aspects are concerned this simplification will not substantially modify the validity of our observations for the more complicated model.

For a classical spin $\vec{S}$, the model (1) can be solved exactly for $U = 0$.[29,30] The result for the single-particle Green function of the d states is

$$G_d(z) = \frac{1}{2} \left(\frac{1}{z - \epsilon_d + i\Delta_0 + J_K} + \frac{1}{z - \epsilon_d + i\Delta_0 - J_K} \right) \quad (2)$$

where $\Delta_0 = \pi N_F V^2$ and we assumed $|\vec{S}|^2 = 1$ and a flat conduction density of states (DOS) of infinite width and value N_F. The resultant DOS $\rho_d(\omega) = -\frac{1}{\pi} \Im m G_d(\omega + i\delta)$ shows two peaks of width Δ_0 centered at $\epsilon_d \pm J_K$. Note that one can view this result as spin-averaged DOS of the SIAM at $U = 0$ in a magnetic field J_K and that the result is independent of the sign of J_K.

III. RESULTS

A. Classical limit

Neither for a quantum spin nor for a classical spin and $U > 0$ an exact solution exists. However, it is tempting to extend the above interpretation for a classical spin in

the following way: Solve a standard SIAM in a magnetic field of J_K and average over the resulting spectra for spin up and down. Note that this procedure again leads to results that do not depend on the sign of J_K.

Since the additional spin enters only on the local level, we use the standard NRG algorithm[18,31,32] to solve the impurity problem and calculate physical quantities. To obtain reliable spectra in a magnetic field, we furthermore employ the technique proposed by Hofstetter.[33] Since a discretization of the energy axis introduced in the NRG leads to discrete spectra, a broadening must be introduced to obtain smooth results for dynamical quantities. Again, we follow the standard procedure here.[31]

As example we present in Fig. 1 calculations for the SIAM in a magnetic field, averaged over the spin direc-
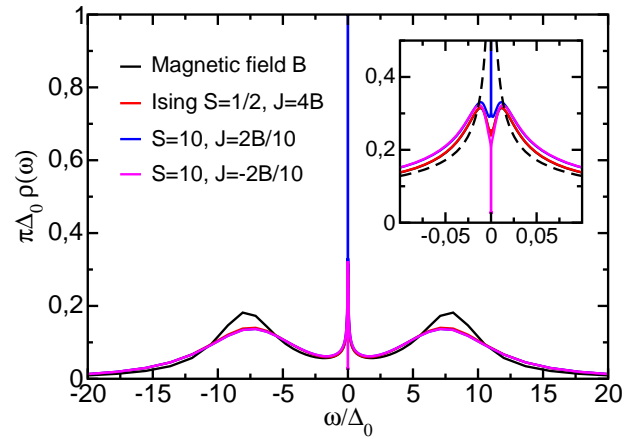

FIG. 1: Impurity DOS for SIAM in a magnetic field, with Ising spin $S = 1/2$ and "classical" spin $S = 10$. For the latter results for both antiferromagnetic and ferromagnetic coupling are shown. The inset displays an enlarged view of the region around $\omega = 0$. The dashed black curve is the result for $S = 0$ and $B = 0$.

tion, together with results for the SIAM with additional Ising respectively classical spin. The parameters for the SIAM are $U/\pi\Delta_0 = 5.3$ and $\epsilon_d = -U/2$, i.e. particle-hole symmetry. The NRG discretization parameter was $\Lambda = 2.5$ and we kept $1000 \ldots 4000$ states per iteration depending on the size of the local spin. The NRG-spectra finally were broadened with a width $b = 0.6$.

The black curve in Fig. 1 was obtained from a calculation with a magnetic field $B = 8 \cdot 10^{-3}\Delta_0$, the red curve with a local Ising spin $S = 1/2$ and coupling $J_K = 4B$, the blue and magenta curves with local spin $S = 10$ and couplings $J_K = \pm 2B/10$ to simulate the classical limit $S \to \infty$. The values of J_K were scaled such that $B = J_K s_d S$. The inset shows an enlarged view of the region around $\omega = 0$; for comparison, the dashed black curve represents the spectrum for $S = 0$, $B = 0$.

While the position of the Hubbard bands at higher energies coincides for all curves, the distribution of spectral weight comes out different for $S > 0$ compared to the case with magnetic field and $S = 0$. This deviation is a

purely numerical effect related to the the differences in the distribution of spectral weight in the Hubbard bands for the discrete NRG spectra with and without applied magnetic field and the broadening introduced to obtain smooth spectra.

In the region around $\omega = 0$ the calculation with Ising spin and magnetic field coincide perfectly, yielding a splitting of the original Kondo resonance at $B = J_K = 0$, as expected. However, the "classical limit" with $S = 10$ differs considerably. Depending on the sign of J_K, either a Kondo resonance (ferromagnetic coupling) or a gap (antiferromagnetic case) emerges at $\omega = 0$ in addition to the splitting of the original Kondo peak. Apparently, even for such a large value of S the effect of quantum fluctuations is still prominent. However, the corresponding energy scales are considerably reduced compared to $J_K = 0$ and we expect the results to converge to the anticipated one as $S \to \infty$.

B. Quantum spins: $S = 1/2$

Let us now turn to the discussion of the effects of a local quantum spin on the low-energy properties. In Fig. 2 the
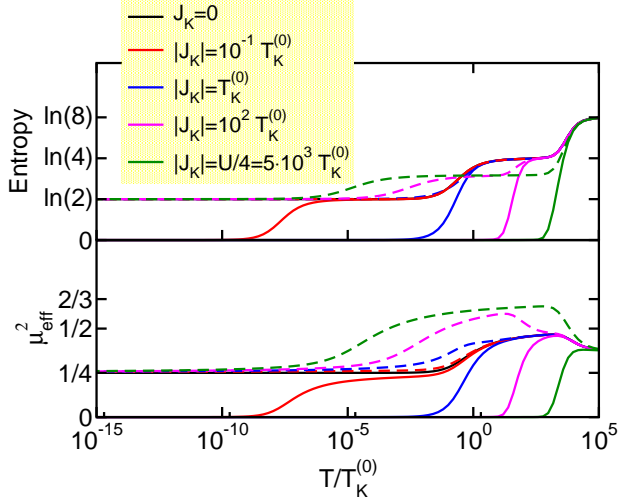
FIG. 2: Entropy and effective impurity moment for different values of J_K as function of $T/T_K^{(0)}$. Full (dashed) lines denote antiferromagnetic (ferromagnetic) coupling.

impurity contribution to the entropy (upper panel) and the effective impurity moment $\mu_{\text{eff}}^2 := T \cdot \chi_{\text{imp}}$ (lower panel) for different values of J_K for a local spin $S = 1/2$ are shown as function of $T/T_K^{(0)}$, where $T_K^{(0)}$ denotes the Kondo scale for the system with $S = 0$. The SIAM parameters were $U = 6.4\pi\Delta_0$ at particle-hole symmetry. The NRG discretization, number of states kept etc. were chosen as before. The full lines in Fig. 2 represent results for antiferromagnetic coupling J_K, the dashed lines those for ferromagnetic coupling.

Decreasing J_K from $J_K = 0$ to some antiferromagnetic $|J_K| < T_K^{(0)}$ results in the scenario depicted by the full red curves in Fig. 2. Around the temperature $T_K^{(0)}$ screening occurs as in the normal Kondo effect, resulting in a situation that resembles a free spin $S = 1/2$ again. For a much lower $T_K \propto T_K^{(0)} \exp\left(-\alpha/(|J_K|/T_K^{(0)})\right)$, a second screening takes place to the ground state with $S = 0$. This latter can be viewed as a conventional Kondo screening of the local spin by the fully formed local Fermi liquid. Hence, the factors $T_K^{(0)}$ appearing in the formula for T_K, representing the effective bandwidth respectively DOS at the Fermi level of the quasi-particles of the local Fermi liquid playing the part of the "conduction states". This effect has been observed before by several authors[25,26,27] and baptized two-stage Kondo screening. When J_K becomes of the order of $T_K^{(0)}$, the Kondo screening is replaced by the formation of a local singlet with an energy scale $\approx |J_K|$.

For ferromagnetic coupling $J_K > 0$, on the other hand, the proper fixed point is – as in the conventional Kondo model – the local-moment one with residual entropy $\ln(2)$ and effective moment $1/2$. Again, from the dashed curves in Fig. 2 one can distinguish two regimes. For $J_K < T_K^{(0)}$ we observe screening on the scale of $T_K^{(0)}$, the additional local spin effectively behaving like a free spin all the way down to $T = 0$. However, for $J_K \gg T_K^{(0)}$ the impurity first forms a local spin triplet (entropy $\ln(3)$ and moment $2/3$). This moment is then partially screened at a reduced Kondo scale $T_K \ll T_K^{(0)}$; energy scales and physical properties will behave as in the conventional underscreened Kondo model.[34,35]
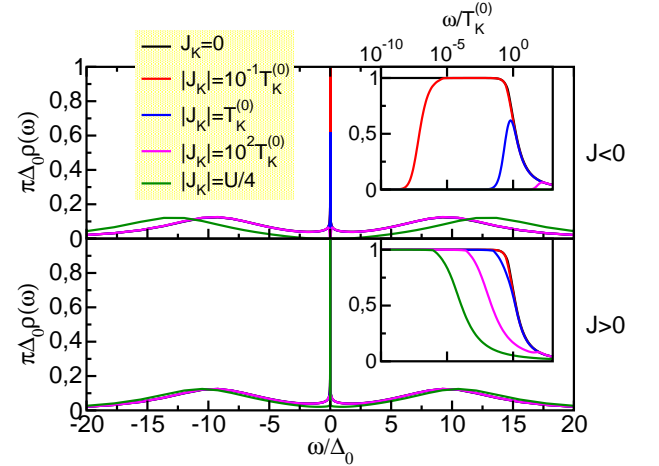
FIG. 3: Local DOS for different values of J_K as function of ω/Δ_0. The insets show the spectra for $\omega > 0$ in a semi-logarithmic plot.

The behavior discussed previously is reflected in the local density of states (DOS) depicted in Fig. 3. As already noted in the classical limit, the coupling to the

additional spin leads to a corresponding shift of the up-
per Hubbard band, which however is for larger $|J_K|$ more
pronounced for antiferromagnetic exchange. In this case
on also nicely sees the two-stage screening at $|J_K| < T_K^{(0)}$
and the formation of the local singlet at $|J_K| > T_K^{(0)}$ (inset
to upper panel of Fig. 3), suppressing the Kondo screen-
ing. Here, one always finds a gap in the DOS at $\omega = 0$,
which size is set by T_K. For ferromagnetic coupling, on
the other hand, the inset in the lower panel of Fig. 3
proves that the screening resonance remains intact, but
shows a width decreasing with increasing J_K.

C. Quantum spins: General S

How does the behavior discussed in the previous sec-
tion change with increasing spin quantum number S_I or
more precisely, do we recover a "classical" result for large
enough S_I? Let us start with a discussion of the weak-
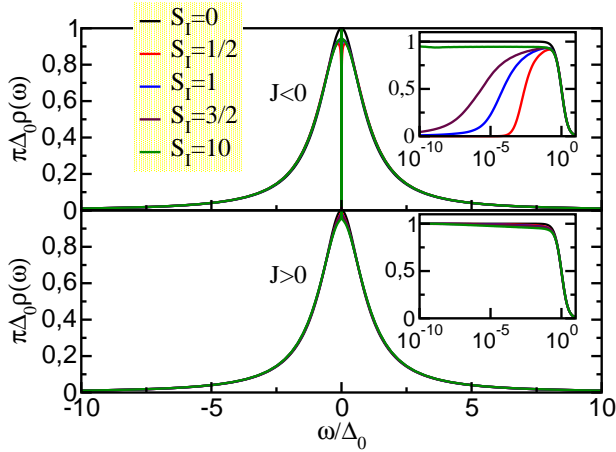coupling results shown in Fig. 4. The calculations were

FIG. 4: Local DOS for fixed $\sqrt{S_I(S_I+1)}|J_K|/\Delta_0 = 1/3$ as
function of ω/Δ_0 in the weak-coupling regime $U/\Delta_0 = 1$ for
different values of local spin S_I. The upper panel collects the
results for antiferromagnetic coupling, the lower panel those
for ferromagnetic. The insets show the spectra for $\omega > 0$ in a
semi-logarithmic plot.

done in the weak-coupling regime $U/\Delta_0 = 1$ for fixed
value $\sqrt{S_I(S_I+1)}|J_K|/\Delta_0 = 1/3$ to achieve the same
classical energy scale for all S_I. We did calculations up
to $S_I = 10$, which, according to our results in section
III A, we expect to be already very close to the classical
limit. Indeed, for $S_I = 10$ (green curves in Fig. 4) we do
find almost identical behavior for $J_K < 0$ and $J_K > 0$ ex-
cept for extremely low temperatures. Note however, that
even for this large value for S_I the DOS for $\omega/\Delta_0 < 0.1$
for $J_K < 0$ does not reach the full unitary limit due to
quantum fluctuations.

The differences are more dramatic for small values of
S_I. As expected, for $J_K < 0$ there occurs a Kondo screen-
ing with an energy-scale $T_K(S_I)$ decreasing exponentially

with increasing S_I. Note that even for comparatively
large $S_I = 3/2$ the influence of quantum fluctuations is
still pronounced and appears in an energy regime that
may still be of experimental relevance.

The differences become even more pronounced if we in-
crease the local Coulomb repulsion to $U/\Delta_0 = 10$, which
lies in the intermediate-coupling regime with a Kondo
scale $T_K^{(0)}/\Delta_0 \approx 0.07$. Since thus $J_K > T_K^{(0)}$ we do not
expect two-stage screening here. The results for oth-
erwise same model parameters are collected in Fig. 5.
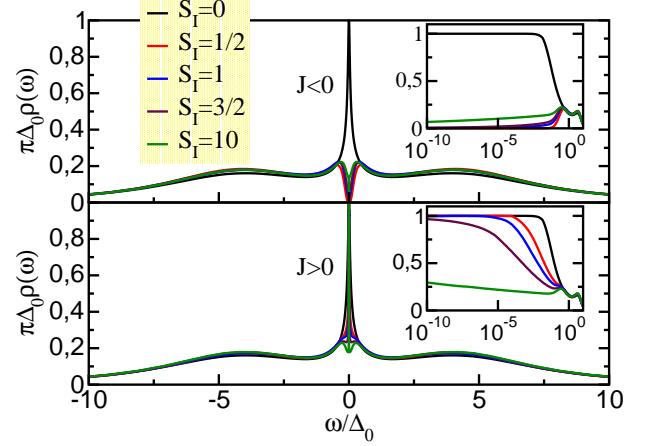Note that due to the choice of J_K the Hubbard bands do

FIG. 5: Local DOS for fixed $\sqrt{S_I(S_I+1)}|J_K|/\Delta_0 = 1/3$
as function of ω/Δ_0 in the intermediate-coupling regime
$U/\Delta_0 = 10$ for different values of local spin S_I. The up-
per panel collects the results for antiferromagnetic coupling,
the lower panel those for ferromagnetic. The insets show the
spectra for $\omega > 0$ in a semi-logarithmic plot.

not move with increasing S_I. Furthermore, in all cases
$S_I > 0$ additional structures appear at $\omega \approx \pm|J_K|$. The
low-energy behavior, however, is markedly different for
$J_K < 0$ (upper panel in Fig. 5) and $J_K > 0$ (lower panel
in Fig. 5). Below $\omega/\Delta_0 < 0.07 \approx T_K^{(0)}$, the former case
always develops a (pseudo-) gap due to the formation of
a singlet between the local degrees of freedom, while the
latter tends to recover a Kondo-resonance for the total
spin, again with exponentially decreasing $T_K(S_I)$. Ow-
ing to the universal behavior of the conventional Ander-
son model for $U/\pi\Delta_o > 1$ ("Kondo regime") we actually
expect the behavior observed here to be generic in this
parameter regime. Quite obviously, while in the weak
coupling regime the "classical limit" is reached already
for moderate values of S_I, one has to be very careful when
dealing with the strongly correlated regime.

IV. SUMMARY AND CONCLUSION

In this paper we presented calculations for an extended
Anderson impurity model, where the local charge degrees

of freedom in addition couple to a localized spin. The motivation to study such a model is based on the observation that in a variety of transition metal or rare earth compounds the complex local orbital structure can be split into a localized spin, which can take large values $S \gg 1/2$, coupled via Hund's exchange to a more delocalized set of possibly also correlated states. A particular example surely is the famous $LaMnO_3$.

The solution of this model for different regimes of model parameters was accomplished by using Wilson's NRG, which provides accurate and reliable results for thermodynamics and dynamics and is able to resolve arbitrarily small energy-scales that may appear in the problem. The findings can be summarized as follows: Even for comparatively large localized spin $S_I = 10$, we still observe the influence of quantum fluctuations on the properties of the impurity charge degrees of freedom. These effects become more pronounced when these charge degrees of freedom are correlated themselves as to be expected for example in $LaMnO_3$. Depending on the ratio $|J_K|/T_K^{(0)}$, where $T_K^{(0)}$ is the Kondo temperature for the model without additional spin, different regimes can be identified, which in contrast to the classical prediction do markedly depend on the sign of J_K.

Thus, for the solution of correlated lattice models with such an additional spin degree of freedom within DMFT one has to be likely careful when using the approximation of a classical spin, even when S_I is comparatively large. Moreover, the expected physics can be read off our results right away, at least for half-filling. Due to the reduced Kondo scale for Hund's type or ferrmomagnetic coupling, we expect a corresponding reduction of a critical U for a Mott-Hubbard transition. On the other hand, for antiferromagnetic exchange coupling the corresponding $U_c = 0$ at $T = 0$, because the forming of a local singlet immediately leads to an insulating state.

Quite interesting are also the magnetic properties of the system. Again, we may anticipate from the impurity calculations that antiferromagnetism is still the prevailing magnetic order, but in the vicinity of certain commensurate band fillings we can also expect ferromagnetic order from a corresponding RKKY exchange. These investigations are currently in progress.

[1] M. Imada, A. Fujimori, and Y. Tokura, Rev. Mod. Phys. **70**, 1039 (1998).

[2] J. Hubbard, Proc. Roy. Soc. London A **276**, 238 (1963).

[3] M. C. Gutzwiller, Phys. Rev. Lett. **10**, 159 (1963).

[4] J. Kanamori, Prog. Theor. Phys. **30**, 275 (1963).

[5] A. P. Ramirez, J. Phys.: Condens. Matter **9**, 8171 (1997).

[6] C. Zener, Phys. Rev. **82**, 403 (1951).

[7] K. Held and D. Vollhardt, Phys. Rev. Lett. **84**, 5168 (2000).

[8] S. Yunoki, J. Hu, A. L. Malvezzi, A. Moreo, N. Furukawa, and E. Dagotto, Phys. Rev. Lett. **80**, 845 (1998).

[9] S. Yunoki, A. Moreo, and E. Dagotto, Phys. Rev. Lett. **81**, 5612 ((1998).

[10] M. J. Calderón and L. Brey, Phys. Rev. B **58**, 3286 (1998).

[11] D. P. Arovas and F. Guinea, Phys. Rev. B **58**, 9150 (1998).

[12] E. Müller-Hartmann and E. Dagotto, Phys. Rev. B **54**, 6819 (1996).

[13] Y. Motome and N. Furukawa, Phys. Rev. B **68**, 144432 (2003).

[14] Y. Motome, N. Furukawa, and N. Nagaosa, Phys. Rev. Lett. **91**, 167204 (2003).

[15] T. Hickel and W. Nolting, Phys. Rev. B **69**, 085110 (2004).

[16] A. Georges, G. Kotliar, W. Krauth, and M. J. Rozenberg, Rev. Mod. Phys. **68**, 13 (1996).

[17] K. G. Wilson, Rev. Mod. Phys. **47**, 773 (1975).

[18] H. R. Krishnamurthy, J. W. Wilkins, and K. G. Wilson, Phys. Rev. B **21**, 1003 (1980).

[19] P. W. Anderson, Phys. Rev. **124**, 41 (1961).

[20] A. C. Hewson, *The Kondo Problem to Heavy Fermions*, Cambridge Studies in Magnetism (Cambridge UNiversity Press, Cambridge, 1993).

[21] T.-S. Kim and S. Hershfield, Phys. Rev. B **63**, 245326 (2001).

[22] K. Kang, S. Cho, J.-J. Kim, and S.-C. Shin, Phys. Rev. B **63**, 113304 (2001).

[23] V. Apel, M. Davidovich, E. Anda, G. Chiappe, and C. Busser, Eur. Phys. J. B **40**, 365 (2004).

[24] G. A. Lara, P. A. Ornella, J. Yanez, and E. V. Anda (2004), cond-mat/0411661.

[25] P. Cornaglia and D. Grempel, Phys. Rev. B **71**, 075305 (2005).

[26] R. Žitko and J. Bonča (2005), cond-mat/0510536.

[27] M. Vojta, R. Bulla, and W. Hofstetter, Phys. Rev. B **65**, 140405(R) (2002).

[28] T. Pruschke and R. Bulla, Eur. Phys. J. B **44**, 217 (2005).

[29] N. Furukawa, J. Phys. Soc. Jpn. **63**, 3214 (1994).

[30] N. Furukawa, in *Physics of Manganites*, edited by T. A. Kaplan and S. D. Mahanti (Plenum Press, New York, 1999).

[31] O. Sakai, Y. Shimizu, and T. Kasuya, J. Phys. Soc. Jpn. **58**, 3666 (1989).

[32] R. Bulla, A. C. Hewson, and T. Pruschke, J. Phys.: Condens. Matter **10**, 8365 (1998).

[33] W. Hofstetter, Phys. Rev. Lett. **85**, 1508 (2000).

[34] O. Parcollet and A. Georges, Phys. Rev. Lett. **79**, 4665 (1997).

[35] P. Nozières and A. Blandin, Journal de Physique (Paris) **41**, 193 (1980).